

## Thermal stability of magnetic tunneling junctions with MgO barriers for high temperature spintronics

Xiaoyong Liu<sup>a)</sup>

Micro Magnetics Inc., Fall River, Massachusetts 02720 and Physics Department, Brown University, Providence, Rhode Island 02912

Dipanjan Mazumdar and Weifeng Shen

Physics Department, Brown University, Providence, Rhode Island 02912

B. D. Schrag

Micro Magnetics Inc., Fall River, Massachusetts 02720 and Physics Department, Brown University, Providence, Rhode Island 02912

Gang Xiao

Physics Department, Brown University, Providence, Rhode Island 02912

(Received 22 March 2006; accepted 22 May 2006; published online 11 July 2006)

Thermal stability of MgO-based magnetic tunnel junctions has been investigated from room temperature up to 500 °C, in both the memory and sensor configurations. Junctions showed magnetoresistances of over 200% at room temperature and over 100% at 300 °C. Below 375 °C, the resistance of the parallel state remains constant, while the antiparallel state resistance linearly decreases with temperature. Above that, a rapid increase in the resistance of both states was observed, along with an irreversible loss of magnetoresistance. Junctions in the sensor configuration exhibited a constant sensitivity of 1.0%/Oe at temperatures up to 300 °C before getting degraded.

© 2006 American Institute of Physics. [DOI: 10.1063/1.2219997]

Magnetic tunnel junctions (MTJs) have attracted enormous interest since the discovery of substantial room temperature tunneling magnetoresistance (TMR) in the mid-1990s. Most current MTJ devices use amorphous  $\text{Al}_2\text{O}_3$  as a tunnel barrier, with magnetoresistance (MR) ratio as high as 70% been observed.<sup>1</sup> Recently, much larger MR values were predicted for epitaxial spin tunneling systems.<sup>2-4</sup> *Ab initio* calculations show that MR values over 1000% are possible in perfectly ordered (100)-oriented single-crystalline Fe/MgO/Fe MTJ trilayers, due to the coherent tunneling properties of electrons with  $\Delta_1$  symmetry in a MgO barrier. Similar calculations on bcc Co/MgO/Co and FeCo/MgO/FeCo structures predicted even larger magnetoresistance values. The experimental confirmations of these theoretical predictions were independently reported by groups from Japan and IBM in 2004, with measured MR values of 220% and 180%, respectively, at room temperature (RT).<sup>5,6</sup> The latter result was more practically significant, because it utilized the more common magnetron sputtering technique instead of molecular beam epitaxy (MBE) for junction deposition. Last year, Djayaprawira *et al.* reported<sup>7</sup> a slightly higher MR of 230% using CoFeB for the electrode material. This value was later improved to 355%.<sup>8</sup> These dramatic improvements in performance achieved using MgO-based MTJs have revitalized the field of spintronics.

On the other hand, thermal stability study of MTJs is of significance, due to compatibility issues with existing complementary metal-oxide semiconductor (CMOS) processes (i.e., for the production of magnetic random access memory) and for sensor applications where high-temperature operation can be important. Previous studies<sup>9-11</sup> related to MTJ thermal stability have mainly focused on the effects of

high-temperature thermal annealing on room temperature junction performance. There are also some reports<sup>12-14</sup> on the operating temperature dependence of MTJ devices, but these are mainly on the low temperature region (below 25 °C). It is the focus of this study to investigate the performance of MgO-based junctions in both the memory and sensor configurations at operating temperatures of up to 500 °C.

The layer structure used for this work was (thicknesses in angstroms): Ta(300)/Co<sub>50</sub>Fe<sub>50</sub>(30)/IrMn(150)/Co<sub>50</sub>Fe<sub>50</sub>(20)/Ru(8)/Co<sub>40</sub>Fe<sub>40</sub>B<sub>20</sub>(30)/MgO(12)/Co<sub>40</sub>Fe<sub>40</sub>B<sub>20</sub>(30)/Ta(100)/Ru(50). Samples were deposited onto a thermally oxidized Si wafer via sputtering. An artificial antiferromagnetic CoFe/Ru/CoFeB trilayer structure has been used for the purpose of increasing exchange bias and thermal stability enhancement (separating the IrMn layer from the MgO barrier is important because Mn atoms can diffuse into the barrier at higher temperatures). The choice of CoFeB for the ferromagnetic (FM) electrodes is not only to improve magnetoresistance but also to serve as diffusion barrier for Mn. Details regarding sample fabrication and optimization are reported elsewhere.<sup>15</sup>

Junctions were patterned into ellipses with lateral dimensions ranging from 2 to 6  $\mu\text{m}$ . Postprocessing thermal annealing was then performed in vacuum at a temperature of 375 °C for 1 h with an applied field of 2.5 kOe. Two types of junctions with different magnetic configurations were fabricated. Junctions in the memory configuration were annealed such that the magnetization of the pinned layer was parallel to the easy axis of free layer. Junctions in the sensor configuration had the pinned layer magnetization set perpendicular to the free layer's easy axis. Transport measurements were done using a dc four point method in a probe station with a heated stage.

<sup>a)</sup>Electronic mail: liu@micromagnetics.com

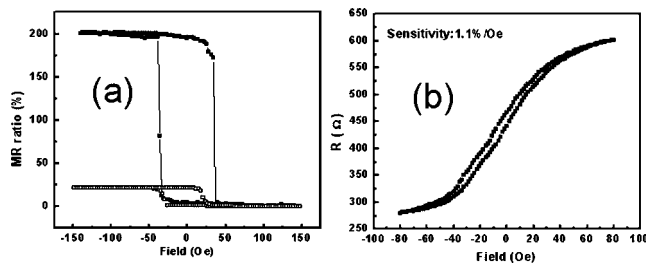


FIG. 1. (a) As-deposited (open circles) and annealed (solid circles) room temperature magnetoresistances as a function of applied field along the free layer easy axis. The bias across the junction is 5 mV. (b) Typical MR transfer curve for a junction fabricated in the sensor configuration.

In Fig. 1(a) we present minor magnetoresistance transfer curves measured at RT for memory-configuration samples before and after annealing. As-deposited MR values are typically 20%–35%, while properly annealed samples consistently show MR of average 200%. Selected samples measured at 4.2 K yielded MR values near 280% (data not shown here). Using Julliere's formula, these data give a spin polarization value of 0.68–0.76 for CoFeB, which agrees well with previous results obtained from *S/I/M* tunneling spectroscopy.<sup>6</sup> For junctions in sensor configuration, a Co-PrCr permanent magnet (PM) film is patterned near active junction area to introduce a longitudinal biasing field in the easy-axis direction. This field reduces domain wall effects and hysteresis in the MR transfer curve, as shown in Fig. 1(b). This figure reveals that sensor-configuration junctions respond to external fields via coherent rotation with a nearly linear response in applied fields of less than 100 Oe. Sensitivity, defined as the slope of sensor transfer curve divided by the device resistance, is about 1.1%/Oe at zero field for these sensors. This is about twice as large as what is obtained in optimized GMR sensors.<sup>16</sup>

To evaluate the influence of temperature on the magnetic properties of our junctions, we measured the MR curves at temperatures ranging from RT to 500 °C. Figure 2(a) shows the MR ratio (normalized with respect to the RT value) as a function of temperature for a typical junction in the memory configuration. The MR decreases steadily with increasing temperature, reaching half of its RT value at ~300 °C. It drops more rapidly thereafter, and a complete loss of MR occurs at ~500 °C. A detailed examination of the transfer curves (not shown here) shows that the exchange bias drops more rapidly with temperature than the MR ratio: the exchange bias is totally lost at 400–450 °C, while the MR ratio in this temperature range is still significant (~20%). This high-temperature stability (400 °C) has not been reported previously by any group. The short-term operating stability of these devices was also investigated in a brief “stress test.” Junctions were operated at a voltage bias of 20 mV continually at 250 °C in an ambient atmosphere for 50 h. No degradation in junction characteristics was observed over this period.

Figure 2(b) shows the variation of junction resistance-area (*RA*) product in both the parallel (*P*) and antiparallel (*AP*) states, as a function of temperature. The insulator-like temperature dependence suggests a direct tunnel process through the barrier and no signs of electron hopping were observed.<sup>17</sup> The decline in MR is largely due to the steady decrease of the *AP* state resistance (the *P* state remains constant, with less than 5% variation from RT to 350 °C). This

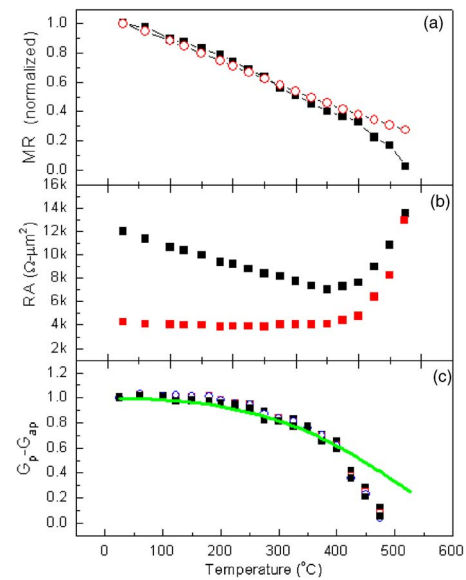


FIG. 2. (Color online) (a) Temperature dependence of normalized magnetoresistance (black squares) with theoretical fitting results (open circles); (b) Dependence of resistance-area product of junctions in the parallel (red) and antiparallel (black) states; (c) Change of conductance of four junctions (normalized at room temperature) along with theoretical fitting (solid line).

behavior, which has been observed in the low-temperature regime,<sup>6</sup> is different from measurements reported for junctions with amorphous  $\text{Al}_2\text{O}_3$  barriers, where both  $R_P$  and  $R_{AP}$  decrease with temperature. Because of the different symmetries of wave functions across the MgO barrier, majority spin channel tunneling dominates the overall conductance in *P* state; while in *AP* state, minority spins tunnel through interface resonance states, and hence have stronger temperature dependence. Additionally, the increase of magnetic disorder with temperature should lower  $R_{AP}$ , but increase  $R_P$ , the coincident cancellation of above two effects gives a much weaker dependence of resistance in *P* state.<sup>6</sup>

The above temperature dependence behavior can be understood empirically using a model proposed by Shang *et al.*<sup>12</sup> It is assumed that the total conductance  $G$  can be modeled as the sum of a spin-dependent ( $G_T$ ) and a spin-independent ( $G_I$ ) component as  $G = G_T[1 + P^2 \cos(\theta)] + G_I$ , where  $\theta$  is the angle between the magnetization of two FM electrodes (CoFeB, in our case). The parameter  $P$  denotes the electrode spin polarization, whose temperature dependence can be assumed to follow the temperature dependence of electrode magnetization  $P(T) = P_0(1 - bT^\alpha)$ , where  $b$  is a constant and  $1 < \alpha < 2$ . The variation of conductance between the two states  $\Delta G = 2G_T P^2$  depends on the temperature dependence of  $P$  and  $G_T$ , where  $G_T = G_0 CT / \sin(CT)$  [ $G_0$  is a constant,  $C = 1.387 \times 10^{-4} d / \sqrt{\phi}$  with barrier width ( $d$ ) in Å, and height ( $\phi$ ) in eV]. The fitting results of  $\Delta G$  are shown in Fig. 2(c) for several different junctions. In addition, Fig. 2(a) contains a theoretical curve showing the expected variation in magnetoresistance with temperature based on fitting parameters in Fig. 2(c). Both curves agree well with our experimental data at temperatures from RT to 350 °C. The discrepancy at higher temperatures may be primarily due to loss of exchange bias, which leads to an underestimation of the *AP* resistance, and hence a faster drop of  $\Delta G$ .

At temperatures above 350 °C, we observed an almost exponential rise in the resistances of both the parallel and

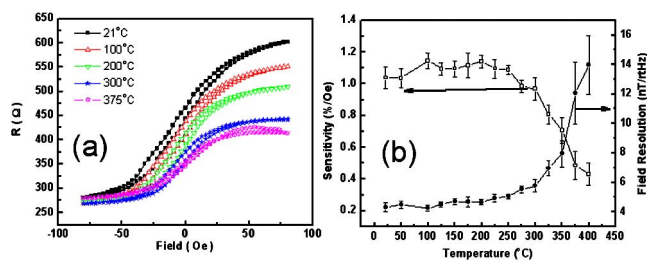


FIG. 3. (Color online) (a) Temperature dependence of the transfer curves of a sensor-configuration junction. (b) Sensitivity (open squares) and estimated magnetic field resolution (solid circles) of the same MTJ sensor as a function of temperature.

antiparallel states [Fig. 2(b)]. The fitted activation energies for this exponential increase were found to be 0.33 and 0.56 eV, for the P and AP states, respectively. The observed temperature dependence cannot be explained by conventional metallic properties, because transfer curves measured after the junctions were heated to 500 °C and cooled down to room temperature showed that the increase in resistance and loss of MR were permanent. The mechanism for the increase of resistance is not clear; it may be related to boron diffusion into the barrier at high temperatures. Recent x-ray photoelectron spectroscopy (XPS) studies<sup>18</sup> have observed boron and boron oxide near or inside the MgO barrier for MgO-based junctions after high-temperature annealing. This explanation is consistent with our data, as the formation of boron oxide would increase tunneling resistance while degrading MR through a disruption of the coherent tunneling processes occurring in the barrier. However, further experiments are needed to conclusively prove this explanation.

Figure 3(a) shows the transfer curve of a typical junction in the sensor configuration measured at different temperatures. As the temperature is increased, the sensor maintains a smooth, linear response but with a gradually decreasing MR value (due to the same reasons discussed above). When the junction temperature is above 375 °C, the response becomes slightly more hysteretic, and Barkhausen jumps, due to irreversible domain wall motion, can be seen. These phenomena can be understood qualitatively as follows. To obtain a favorable sensor response, it is necessary to create conditions in which the MTJ will switch its orientation via coherent rotation. This is realized by the introduction of PM biasing. In spite of weakening of PM biasing field with temperature, it is still strong enough to maintain an orthogonal alignment, hence a linear response. But when the temperature is further increased, highly hysteretic domain wall motion may contribute. This critical temperature (in our case about 375 °C) is related to the thickness, magnetization, and magnetic properties of PM materials. We have plotted the sensor sensitivity as a function of temperature in Fig. 3(b). It is interesting that the sensitivity is essentially constant at  $\sim 1\%$ /Oe between RT and 275 °C, before decreasing at higher temperatures.

This occurs because the sensitivity scales as the ratio of magnetoresistance over the zero-field resistance. Since both of these linearly decrease with temperature, a constant sensitivity is achieved over a wide range of temperatures.

Noise measurements of junctions on the same wafer showed that sensor noise is dominated by Johnson noise and shot noise at high frequency region (up to 51 kHz of system bandwidth) with a crossover to  $1/f$ -like noise below 2 kHz. Based on the sensitivity data, and assuming that the temperature dependence of noise at high frequency follows the temperature dependence of Johnson noise, the magnetic field resolution of the sensor (the ratio of voltage noise to that of voltage sensitivity) can be estimated.<sup>19,20</sup> As seen in Fig. 3(b), the minimal detectable magnetic field slowly increases with temperature from 4 nT/rHz at RT to just under 6 nT/rHz at 300 °C, indicating good temperature stability.

The authors are grateful to Xiaohang Zhang for low-temperature measurement, and Dr. Cong Ren for fruitful discussions. This work was supported by the NSF through Grant No. DMR-0306711 and by the ATP program of NIST.

<sup>1</sup>D. Wang, C. Nordman, J. Daughton, Z. Qian, and J. Fink, *IEEE Trans. Magn.* **40**, 2269 (2004).

<sup>2</sup>W. H. Butler, X.-G. Zhang, T. C. Schulthess, and J. M. MacLaren, *Phys. Rev. B* **63**, 054416 (2001).

<sup>3</sup>J. Mathon and A. Umerski, *Phys. Rev. B* **63**, 220403R (2001).

<sup>4</sup>X.-G. Zhang and W. H. Butler, *Phys. Rev. B* **70**, 172407 (2004).

<sup>5</sup>S. Yuasa, T. Nagahama, A. Fukushima, Y. Suzuki, and K. J. Ando, *Nat. Mater.* **3**, 868 (2004).

<sup>6</sup>S. S. P. Parkin, C. Kaiser, A. Panchula, P. M. Rice, B. Hughes, M. Samant, and S.-H. Yang, *Nat. Mater.* **3**, 862 (2004).

<sup>7</sup>D. D. Djayaprawira, K. Tsunekawa, M. Nagai, H. Maehara, S. Yamagata, and N. Watanabe, *Appl. Phys. Lett.* **86**, 092502 (2005).

<sup>8</sup>S. Ikeda, J. Hayakawa, Y. M. Lee, R. Sasaki, T. Meguro, F. Matsukura, and H. Ohno, *Jpn. J. Appl. Phys., Part 2* **44**, L1442 (2005).

<sup>9</sup>R. C. Sousa, J. J. Sun, V. Soares, P. P. Freitas, A. Kling, M. F. da Silva, and J. C. Soares, *Appl. Phys. Lett.* **73**, 3288 (1998).

<sup>10</sup>S. Cardoso, R. Ferreira, P. P. Freitas, P. Wei, and J. C. Soares, *Appl. Phys. Lett.* **76**, 3792 (2000).

<sup>11</sup>N. Matsukawa, A. Odagawa, Y. Sugita, Y. Kawashima, Y. Morinaga, M. Satomi, M. Hiramoto, and J. Kuwata, *Appl. Phys. Lett.* **25**, 4784 (2002).

<sup>12</sup>C. H. Shang, J. Nowak, R. Jasen, and J. S. Moodera, *Phys. Rev. B* **58**, R2917 (1998).

<sup>13</sup>P. Wisniewski, T. Stobiecki, M. Czapkiwicz, J. Wrona, M. Rams, C. G. Kim, C. O. Kim, Y. K. Hu, M. Tsunoda, and M. Takahashi, *Phys. Status Solidi A* **201**, 1648 (2004).

<sup>14</sup>K. I. Lee, J. H. Lee, W. L. Lee, K. H. Shin, Y. B. Sung, J. G. Ha, K. Rhie, and B. C. Lee, *J. Appl. Phys.* **91**, 7959 (2002).

<sup>15</sup>W. Shen, D. Mazumdar, X. Zou, X. Liu, B. D. Schrag, and G. Xiao, *Appl. Phys. Lett.* **88**, 182508 (2006).

<sup>16</sup>A. Veloso and P. P. Freitas, *Appl. Phys. Lett.* **87**, 5744 (2000).

<sup>17</sup>J. J. Akerman, R. Escudero, C. Leighton, S. Kim, D. A. Rabson, R. W. Dave, J. M. Slaughter, and K. Schuller, *J. Magn. Magn. Mater.* **240**, 86 (2002).

<sup>18</sup>J. Y. Bae, W. C. Lim, H. J. Kim, T. D. Lee, K. W. Kim, and T. W. Kim, *J. Appl. Phys.* **99**, 08T316 (2006).

<sup>19</sup>M. Tondra, J. M. Daughton, D. Wang, R. S. Beech, A. Fink, and J. A. Taylor, *J. Appl. Phys.* **83**, 6688 (1998).

<sup>20</sup>C. Ren, X. Liu, B. Schrag, and G. Xiao, *Phys. Rev. B* **69**, 104405 (2005).